APPLIED GEOPHYSICS, Vol.20, No.4 (December 2023), P. 1−13, 12 Figures.
DOI:10.1007/s11770-023-1044-9

Porosity prediction in tight sandstone reservoirs based on a one–dimensional convolutional neural network–gated recurrent unit model

Shi Su-Zhen[1*], Shi Gui-Fei[2], Pei Jin-Bo[2], Li-Li[2], Zhao Kang[2], and He Ya-Zhou[2]

Abstract: Characterizing reservoir porosity is crucial for oil and gas exploration and reservoir evaluation. Due to the increasing demands of oil and gas exploration and development, characterizing reservoir porosity to the required precision using current methods is challenging. Therefore, this study proposes a Pearson correlation–random forest (RF) scheme to select optimal seismic attributes for predicting reservoir porosity and a one-dimensional convolutional neural network–gated recurrent unit (1D CNN–GRU) joint model for reservoir porosity prediction based on well logs and seismic attribute data. First, Pearson correlation–RF is used to select the optimal combination of seismic attribute data suitable for network training. The model learns the nonlinear mapping between porosity logs at well sites and seismic attribute data. It can precisely predict three-dimensional porosity volumes by extending these mappings to nonwell areas. By performing tests near a tight sandstone reservoir, the predicted porosities of the proposed 1D CNN–GRU joint model were a better fit for true porosity values than those of single-network models. Furthermore, the proposed model obtained a laterally contiguous description of the shape and porosity distribution of the tight sandstone reservoir. By integrating advanced machine learning techniques with seismic data analysis, this method provides new approaches and ideas for wide-area porosity predictions for tight sandstone reservoirs using seismic data and opens up possibilities for more detailed and accurate subsurface mapping.
Keywords: Porosity prediction; attribute selection; random forest; convolutional neural network; gated recurrent unit

Introduction

Porosity is an important parameter for reservoir characterization because it directly indicates the ability of a reservoir to store hydrocarbons. Moreover, porosity prediction is important in delineating, characterizing, and evaluating reservoirs and well site selection. Therefore, accurate estimation of reservoir porosity is crucial.

Currently, the most commonly used methods for reservoir porosity characterization are petrophysical tests on core samples and linear equation–based and artificial intelligence (AI)-based porosity prediction. Bakhorji et al. (2012) and Agbadze et al. (2022) suggested that petrophysical tests provide the most accurate assessments of porosity because geological factors, such as tectonic settings and lithological variations, easily influence reservoir porosity. However, this approach

Manuscript received by the Editor August 27, 2023; revised manuscript received November 12, 2023
1. State Key Laboratory for Fine Exploration and Intelligent Development of Coal Resources, China University of Mining and Technology-Beijing, Beijing, 100083, China
2. College of Geoscience and Surveying Engineering, China University of Mining and Technology-Beijing, Beijing 100083, China
*Corresponding author: Shi Su-zhen (E-mail: ssz@cumtb.edu.cn).

is impractical for large-scale applications because the acquisition costs of core samples are exceptionally high and performing porosity measurements on core samples is challenging (Haskett, 1988; Farquhar, 1994). Because porosity is intrinsically related to pore-throat radius and seismic velocity, predicting reservoir porosity using well logs is possible (Zhang, 2023). Empirical equations are used in this approach to extract empirical parameters from density, acoustic, and compensated neutron logs based on local conditions (Jaf, 2015). This approach has been extensively studied inside and outside of China. For instance, Wyllie et al. (1956) proposed a time-average equation for predicting reservoir porosity; however, it is only suitable for geologically simple regions. Raymer et al. (1980) improved this time-average equation, enabling its use in more complex geological conditions. Hampson et al. (2001) used multivariate regression to predict the porosity of geologically simple sandstone reservoirs, yielding a respectable level of predictive accuracy. Based on acoustic impedance inversion and seismic attributes, Pramamik et al. (2004) used multilinear regression to analyze the porosity of ordinary sandstone reservoirs. However, due to the advances in oil and gas exploration technology, porosity predictions based on linear regression are no longer considered sufficiently accurate to meet today's requirements. Therefore, determining reasonable nonlinear mappings between seismic data and porosity is necessary to address this problem.

Recent advances in AI have made using machine learning for reservoir parameter prediction possible. The algorithm learns the nonlinear relations between porosity and other inputs to predict reservoir porosity. The machine learning algorithms used for this purpose are simple shallow networks, such as random forest (RF) (Zou, 2021), support vector machines (Al-Anazi, 2012; Na'imi, 2014), backpropagation (Hamidi, 2012; Zhang, 2021), and artificial neural networks (Duan, 2016; Al Moqbel 2011; Liu 2022). Currently, these models are used by scholars worldwide for porosity predictions.

Recently, deep learning has increasingly been used for reservoir porosity prediction, and deep learning algorithms have outperformed traditional machine learning algorithms in this field. Currently, multiple studies on porosity prediction are being performed using deep learning networks. For instance, Srisutthiyakorn (2016) combined petrographic thin sections with deep learning to develop a porosity estimation method. Feng et al. (2020) used a convolutional neural network (CNN) model to predict reservoir porosity. Chen et al. (2020) and An et al. (2019) used the long short-term memory (LSTM) network to predict reservoir porosity from well logs and demonstrated that LSTM is highly robust and accurate for time-series predictions. Wang et al. (2020) and Zhang et al. (2021) used gated recurrent unit (GRU) networks to estimate porosity from well logs, enabling feature extraction from the logs of adjacent wells. Yang et al. (2023) used the LSTM network with a transformer to predict reservoir porosity from well logs. Anh et al. (2023) combined digital elevation model data with LSTM to predict the porosity of riverbed material. Song et al. (2023) used a weighted ensemble of deep neural networks to predict underground porosity from seismic attributes.

To improve the extraction of lateral spatial and time-series features, a one-dimensional (1D) CNN–GRU network was used to learn the complex nonlinear relationships between seismic data and reservoir porosity using well-log porosities as labels. In this joint network, 1D CNN demonstrates an aptitude for discerning localized patterns and features within the data, rendering it well-suited for extracting lateral characteristics from seismic data. Conversely, GRU exhibits heightened sensitivity to temporal dependencies within the data owing to its inherent memory functionality. This 1D CNN–GRU network improved the accuracy and range of reservoir porosity predictions.

Seismic attribute selection using Pearson correlation–RF

When predicting reservoir parameters based on seismic attributes, selecting the seismic attributes that considerably correlate with the reservoir parameter that needs to be predicted is necessary. This is usually achieved by elimination; all seismic attributes that could correlate with reservoir parameters are selected, and the less relevant attributes are successively eliminated. This approach ensures that all information in the seismic data is used, improving predictive accuracy and reducing the tendency of reservoir predictions to produce multiple solutions.

1.1 Pearson correlation analysis

Pearson correlation analysis is used to search for relations between a pair of variables, which can be used to detect linear correlations between sample data. The

mathematical expression of Pearson correlation analysis is as follows:

$$\rho(x,y)=\frac{\sum_{i=1}^{n}\left(x_i-\bar{x}\right)\left(y_i-\bar{y}\right)}{\sqrt{\sum_{i=1}^{n}\left(x_i-\bar{x}\right)^2\left(y_i-\bar{y}\right)^2}}. \quad (1)$$

where x_i and y_i represent the input datasets for correlation analysis, ρ represents the Pearson correlation coefficient, $\bar{x}$ and $\bar{y}$ represent the mean values of the input datasets. In general, the Pearson correlation coefficient lies in the range [−1, 1], with negative values indicating a negative correlation and 0 indicating an absence of linear correlation.

1.2 Feature importance calculations using the RF algorithm

RF is an ensemble algorithm in which multiple decision trees are used to randomly sample a dataset and learn their nonlinear relations. Finally, each tree votes according to its prediction, and the majority vote becomes the final prediction. RF can be used for feature selection because it can compute the importance of each input attribute (feature) for a target parameter, i.e., feature importance.

When the RF algorithm solves a regression problem, feature importance is obtained from calculating out-of-bag (OOB) errors. In a dataset with m samples, OOB refers to data not sampled after each decision tree performed m rounds of random sampling with replacement. For each decision tree i, its OOB set, $OOB1_i$, is used as input to calculate its OOB error, $errorOOB1_i$. When calculating the importance of attribute K, I_K, random noise is added to the numerical values of K within $OOB1_i$ to produce $OOB2_i$, the OOB set with perturbed K. $OOB2_i$ is then inputted into the trained RF model to obtain $errorOOB2_i$ for each tree i.

If there are N decision trees in the RF model, then I_K is obtained as follows:

$$I_k=\frac{\sum_{I=1}^{N}(errorOOB2_i-errorOOB1_i)}{N}. \quad (2)$$

Finally, all I_K values are normalized to obtain the final feature importance values.

1.3 Seismic attribute selection based on Pearson correlation–RF

Tight sandstone reservoirs are strongly heterogeneous, resulting in strong nonlinear correlations between porosity and certain seismic attributes. First, we used Pearson correlation analysis to perform a preliminary screening for candidate seismic attributes because directly searching for nonlinear relations between porosity and seismic attributes is challenging. Typically, nonlinear relation analysis is performed using neural network models; however, using neural networks to directly find mappings between seismic attributes and porosity would be inefficient. Therefore, we used RF to select the most relevant attributes and then used these attributes as training data for a deep learning model. Consequently, a Pearson correlation analysis–RF scheme for seismic attribute selection was established (Fig. 1).

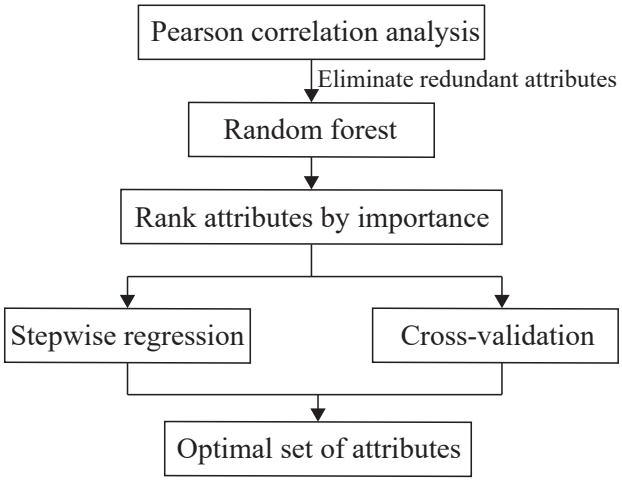

Fig. 1 Attribute selection flow chart.

(1) Pearson correlation analysis calculated the Pearson correlation between each input seismic attribute. The attributes were ranked by their correlation with the porosity curve, and the attributes that strongly correlated with each other and poorly correlated with porosity were excluded. The attributes that remained after excluding redundant attributes were the initial set of selected attributes.

(2) RF calculated feature importance for the attributes selected in Step (1), ranked by importance. Based on stepwise regression, the attributes were grouped according to their importance rankings, and the dataset was partitioned into n parts using n-fold cross-validation. To train the model, the n−1 datasets were the training sets, one after another, whereas the last dataset was the validation set. Finally, the average validation error was treated as the generalized error, and the group of attributes with the lowest error was selected as the dataset for this study.

Reservoir porosity prediction based on the 1D CNN–GRU model

2.1 CNN

The CNN model, proposed by Lecun et al. in 1998, is a powerful feature extraction model. It is one of the most used deep learning networks for classification and regression prediction. Since the CNN architecture has shared weights and local connections, it has fewer parameters and lower complexity than other deep learning networks.

CNNs can be classified as 1D, two-dimensional (2D), and three-dimensional CNNs, depending on the dimensionality and directions of their convolutions. In a 1D CNN, the kernel only moves in one direction; in 2D and 3D CNNs, the kernel moves in two and three directions, respectively (Fig. 2). Currently, regression predictions are primarily performed using 1D CNNs.

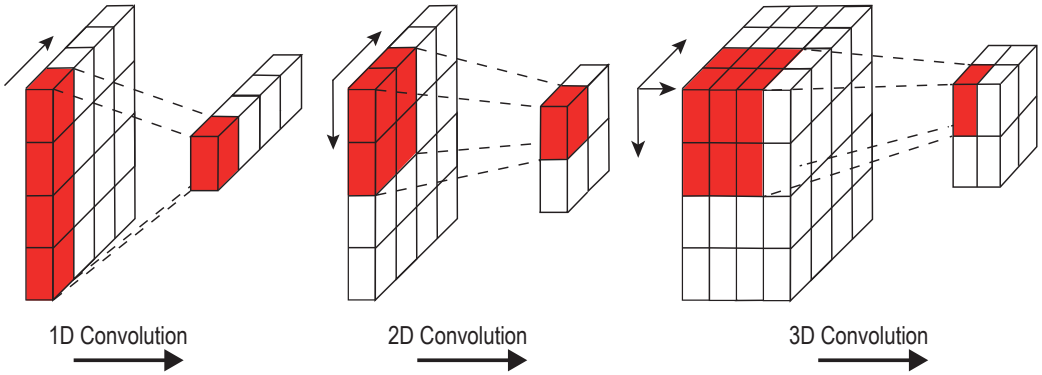

Fig. 2 Illustration of convolutions.

2.2 GRU

Cho et al., in 2014, proposed the GRU network, which is an improved version of the LSTM network. An LSTM unit comprises forget, input, and output gates, allowing the network to decide the time-series information stored and thus control the cell state of the unit (Shi, 2023). In the GRU unit, the three gates of LSTM are replaced by two gates, the reset and update gates.

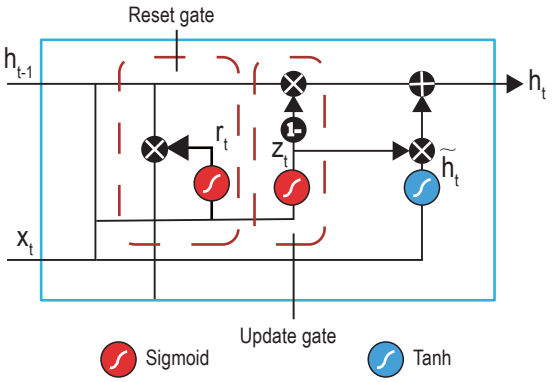

Fig. 3 Architecture of a GRU cell.

Figure 3 depicts the unit structure of a GRU network. The reset gate, r, determines the amount of information from the previous instant in time that should be forgotten, thus helping the network capture short-term dependencies in time-series data. The closer its value is to 1, the less the amount of previous information that is forgotten. This can be mathematically expressed as follows:

$$r_t = \sigma(W_r x_t + U_r h_{t-1} + b_r). \quad (3)$$

The update gate, z, determines how much of the input from the previous state should be used to update the current state, thus helping to capture long-term dependencies in time-series data. The mathematical expression of the update gate is as follows:

$$z_t = \sigma(W_z x_t + U_z h_{t-1} + b_z). \quad (4)$$

Because a GRU cell cannot explicitly determine whether the hidden state should be updated, it uses a candidate hidden state, which is expressed as follows:

$$\tilde{h}_t = \tanh(W x_t + U(r_t \cdot h_{t-1}) + b_h). \quad (5)$$

The current hidden state, h_t, is generated by the candidate hidden state and update gate, z, with the latter controlling the ratio of information in h_t from the previous state h_{t-1} and (new) candidate hidden state $\tilde{h}_t$. After all the information is summed, the final output of the GRU is obtained as follows:

$$h_t = z_t \cdot h_{t-1} + (1 - z_t) \cdot \tilde{h}_t, \quad (6)$$

where x represents the input vector, σ represents the sigmoid activation function, and h_{t-1} represents the hidden state of the GRU cell at time $t-1$. The weight matrices $W \in \boldsymbol{R}^{d\times n}$ and $U \in \boldsymbol{R}^{n\times n}$ are obtained from the training model, with d and n being the number of input samples and hidden units, respectively. The current output of the GRU cell is h_t, and b is the bias term.

Because a GRU network can store information from the previous time step and use it as input for the current instant, it can learn from sequential data and obtain relations between adjacent sampling points at different depths in a well log. GRU networks have a simpler and lighter architecture and fewer network parameters than LSTM networks; therefore, they generally have better training efficiency than LSTM networks.

2.3 1D CNN–GRU joint model

Single deep learning models cannot adequately capture the lateral variation trends of the relation between the input seismic attributes and porosity values with varying depths. CNN is a powerful extractor of local spatial features from input vectors owing to its shared weights and local receptive fields. In contrast, GRU is adept at extracting long-term dependencies because it can selectively retain and forget information according to the sequence characteristics of data. Therefore, we used a 1D CNN–GRU joint model (Fig. 4) for porosity prediction. The 1D CNN first extracts the lateral spatial features of the seismic attributes (well-side seismic data), and the GRU network then extracts their vertical time-series features to obtain spatiotemporal features from seismic data.

In the 1D CNN of our model, modifications were made to the traditional CNN architecture. The sequential data were processed by replacing the convolutional layers in the CNN with 1D convolutions, which are responsible for extracting the multidimensional spatial characteristics of the input features. In a conventional CNN, the pooling layer reduces the dimensions of the high-dimensionality data obtained from convolutions, thereby reducing the amount of data that must be computed and improving training efficiency. However, during mean or max pooling, the location of each feature was not recorded, resulting in the loss of ordering information; the ordered data subsequently became disordered. Furthermore, the fully connected layer, which is meant to map dimension-reduced features from the pooling layer to the label space, disrupts the order of

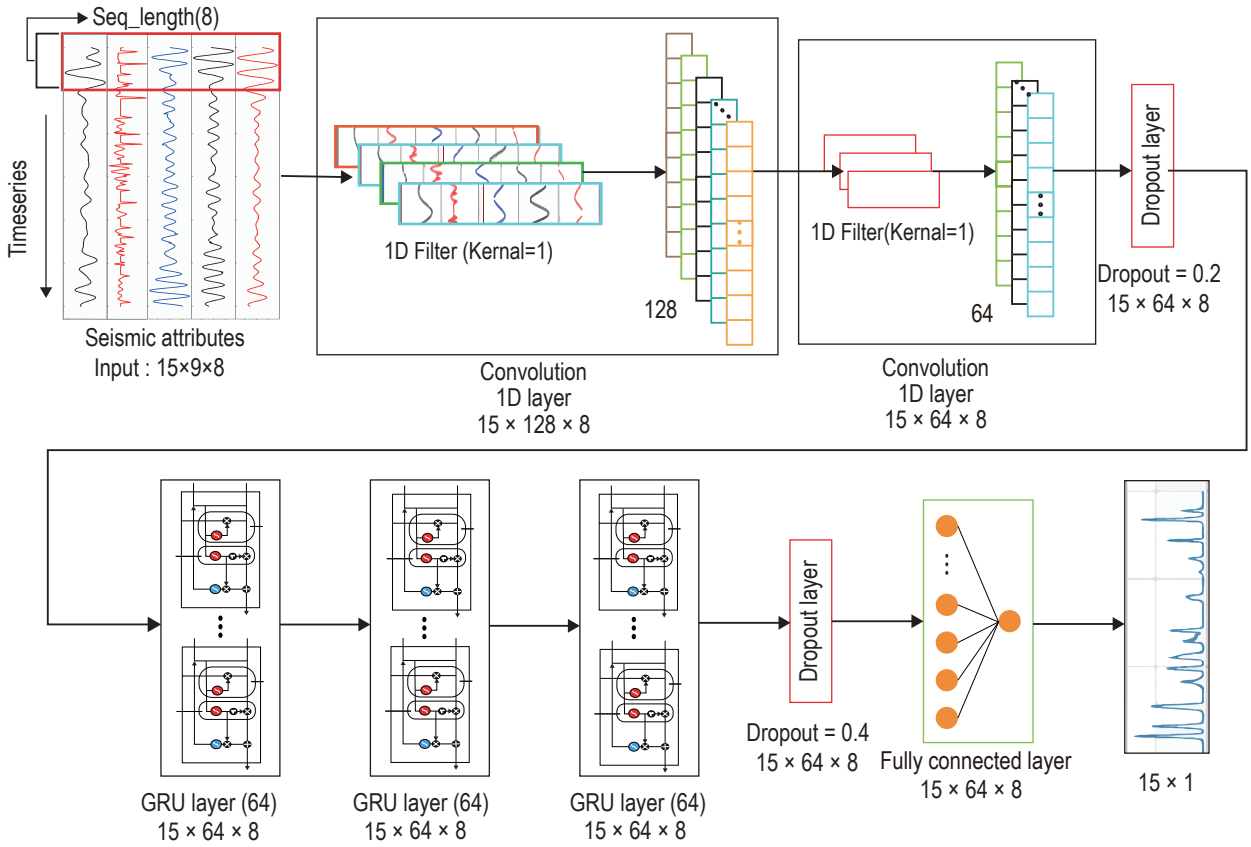

Fig. 4 Architecture of the 1D CNN–GRU model.

data and renders it challenging for the GRU network to extract sequence features.

To address these problems, the pooling and fully connected layers of the 1D CNN were discarded, whereas the 1D convolutional layer, containing extracted spatial features, was retained and placed in front of the GRU network. This modification allows the 1D CNN to extract lateral spatial features from the data without disrupting their vertical (temporal or depth-wise) order, similar to optimizing the training attribute data for the GRU network. Consequently, this modification considerably improved the predictive performance of the 1D CNN–GRU model.

3 Real-world example

3.1 Overview of the study area

Work Area W is in Shenfu, near the eastern edge of the Ordos Basin. It has a classic loess hill landscape with complex terrain and several ravines and gullies. The shape of this region is an NS-trending strip, whose boundaries are defined by the EW-trending Qinling, Yinshan mountain ranges to its south and north, and the NS-trending Shanxi Rift. Therefore, the tectonic deformations of the study area are primarily controlled by NS-trending tectonics. No major tectonic deformations are present in this area. Work Area W is an NS-trending west-dipping monocline with small NS-trending folds and a relatively straightforward tectonic structure. Its strata are relatively flat and even, and no faults are observed in the area.

3.2 Attribute selection based on Pearson correlation–RF

Work Area W contains 12 wells named Jing-1, Jing-2, …, and Jing-12. This study performed porosity predictions for the 1300–2020 m depth range, corresponding to the seventh member of the Shihezi Formation to the second member of the Benxi Formation, in the middle of the well-log deflections using 800–1160 ms seismic data. The well logs for Jing-1–Jing-9 were the training data, and the logs of Jing-10–Jing-11 were the validation set. The well log of Jing-12 was the blind set to evaluate the efficacy of the porosity predictions of the network.

Twenty-one seismic attributes were extracted from the target area, including root-mean-square amplitude (RMS Amp), instant phase, and instant frequency (Instant Freq). Twenty-two initial attribute datasets were created using the original seismic data.

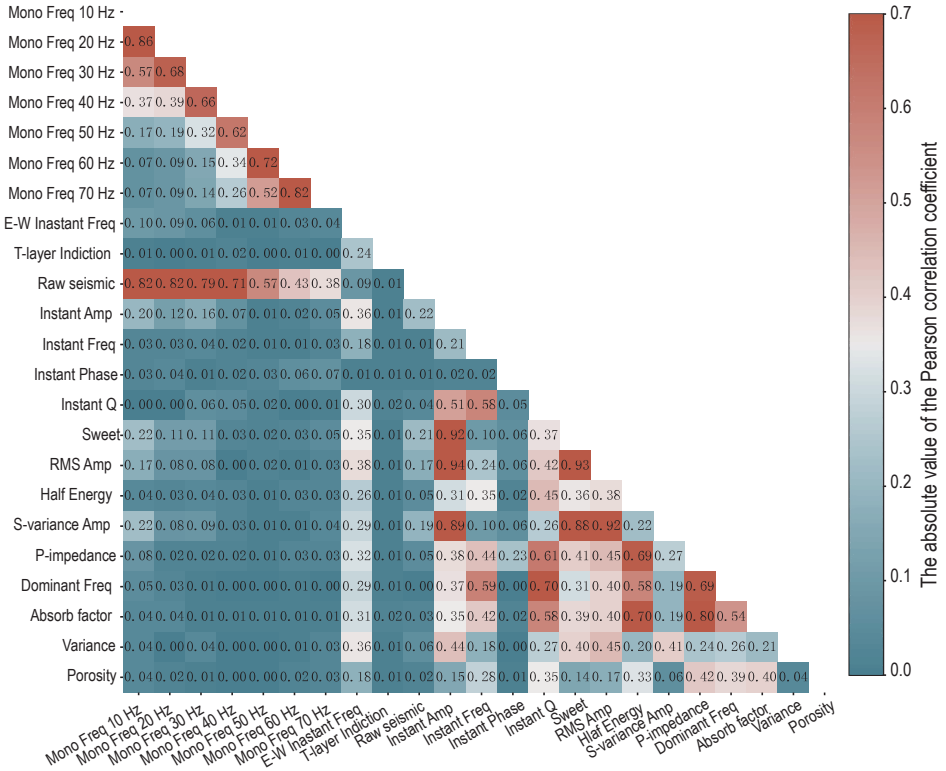

Fig. 5 Pearson correlation coefficient matrix.

Pearson correlation analysis was used to calculate the linear correlation between each attribute and the porosity logs. If a group of attributes strongly correlated with each other (Pearson correlation > 0.8), the attribute with the highest correlation with the porosity log in this group was retained, whereas the remainder were considered redundant and, thus, excluded. Preliminary selection was performed according to the steps above, producing the results in Table 1.

Table 1 Initially selected attributes from Pearson correlation analysis

No.	Features_name	Correlation coefficient
1	P-impedance	0.42
2	Absorb factor	0.40
3	Dominant Freq	0.39
4	Instant Q	0.35
5	Half Energy	0.33
6	Instant Freq	0.28
7	E-W Instant Freq	0.18
8	RMS Amp	0.17
9	Mono Freq 10 Hz	0.04
10	Variance	0.04
11	Mono Freq 70 Hz	0.03
12	Instant Phase	0.01
13	T-layer Induction	0.01
14	Mono Freq 30 Hz	0.01
15	Mono Freq 50 Hz	0.01
16	Mono Freq 40 Hz	0.01

Through this analysis, it can be surmised that the seismic attributes only have weak linear correlations with the porosity log. Therefore, if one attempts to predict porosity using only one or a few seismic attributes, the results will be ambiguous. However, too many attributes would result in an overly complex network. Therefore, RF was used to calculate the importance of the seismic attributes selected via Pearson correlation analysis.

Figure 6 shows the ranking of importance of the attributes obtained from RF. Acoustic impedance (P-impedance), obtained from seismic waveform indicator inversion, has the highest importance (0.276), followed by RMS Amp (0.08) and Mono Freq 10 Hz (0.062). Since the P-impedance accounts for 28% of the total importance, it is the most crucial factor for reservoir porosity prediction. Although establishing a precise importance threshold from this result is impossible, we consequently chose the optimal combination of

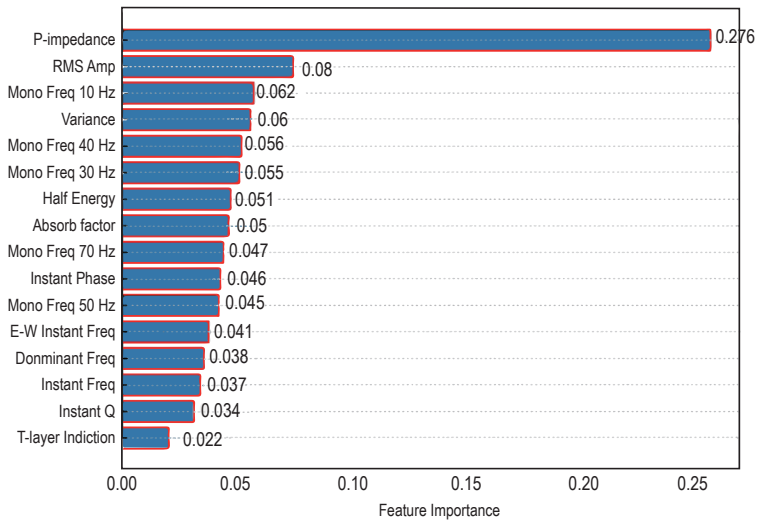

Fig. 6 Ranking of attributes by importance using the RF algorithm.

attributes; ranking attributes by importance provides important clues for selecting an optimal feature set.

The optimal set of attributes was obtained using stepwise regression to group the 16 seismic attributes according to their RF-generated feature importance values, i.e., Attribute Set 1 was defined as P-impedance, Attribute Set 2 as P-impedance and RMS Amp, and Attribute Set 3 as P-impedance, RMS Amp, and Mono Freq 10 Hz. Sixteen sets were created, which were subsequently used as inputs for RF. For each attribute set, 70% of the attribute data were randomly sampled to create the training set of the RF model, whereas the remaining data were used as the validation set. Elevenfold cross-validation was performed to ensure correspondence with the logs of the 11 wells. In each instance, one was the validation well, whereas the remaining were training wells. Finally, the "goodness" of each attribute set was evaluated by averaging the 11 RMS errors (RMSEs), and the attribute set that minimizes the average error was chosen as the optimal attribute set.

Figure 7 shows the average errors of the attribute sets obtained from 11-fold cross-validation. The average error decreased with the number of attributes included in the attribute set, up to nine attributes, where the average error reached its minimum (1.129). Further increases in attributes increased the average error, which eventually stabilized. This result indicates that overfitting occurred in the RF model after nine attributes. Therefore, too many features will decrease predictive performance, increasing computational complexity and wasting time.

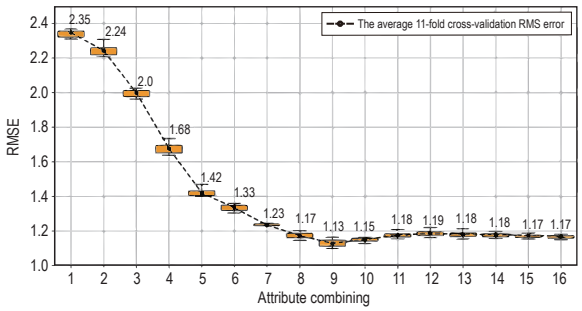

Fig. 7 Results of cross-validation.

Hence, the first nine attributes were selected (Table 2).

Table 2 Final set of attributes

No.	Features_name	Importance
1	P-impedance	0.276
2	RMS Amp	0.080
3	Mono Freq 10 Hz	0.062
4	Variance	0.060
5	Mono Freq 40 Hz	0.056
6	Mono Freq 30 Hz	0.055
7	Half engery	0.051
8	Absorb factor	0.050
9	Mono Freq 70 Hz	0.047

3.3 1D CNN-GRU porosity prediction model

The nine selected seismic attributes were used to train the 1D CNN–GRU joint deep learning network. The deep learning neural network used in this study was based on the Pytorch framework. The risk of overfitting was reduced using the dropout function to tune the number of neurons in the hidden layer. Dropout layers were placed at the last layer of the 1D CNN and after the GRU layer. The hyperparameters of the 1D CNN–GRU network were optimized using the Adam optimizer, which implements the Adam algorithm, to search for the global optimum for training the network. Since this optimizer can adaptively tune the learning rate of the network, a high learning rate can be used initially, decreasing by some ratio after a specific number of epochs. Therefore, the initial learning rate was 0.001, ensuring the network converges quickly without missing the global optimum. After a few training rounds, the network converged around 200–300 epochs. Therefore, the maximum number of epochs was 500. The remaining hyperparameter settings of the 1D CNN–GRU model for reservoir porosity prediction (number of neurons, layers in the 1D CNN network, and hidden layers in the GRU) were determined from repeated trials and our previous experience. Table 3 shows the final configuration of the model.

Table 3 Hyperparameter settings of the 1D CNN–GRU model

Layer_name	Parameters
1D CNN	in_channels = 9; out_channels = 128; stride = 1; kernel_size = 1
1D CNN	in_channels = 128; out_channels = 64; stride = 1; kernel_size = 1; Dropout = 0.2
GRU-1	input_size = 64; hidden_size = 64; Seq_lenth = 8
GRU-2	input_size = 64; hidden_size = 64; Seq_lenth = 8
GRU-3	input_size = 64; hidden_size = 64; Dropout = 0.4; Seq_lenth = 8
FC Layer	in_features = 64; hidden_size = 64; out_features = 1

A detailed explanation of the layers and parameters of the model is provided below.

(1) The input layer processes the attribute data into datasets to train the model. Since nine attributes were chosen, "in_channels" was set to 9.

(2) The 1D CNN layer extracts the lateral spatial features from the input attribute sequences, functioning as input data for the subsequent GRU layer. The 1D CNN was set as two layers to ensure that the lateral spatial features were thoroughly extracted. Disrupting the order of data was prevented using a small kernel size (kernel_size = 1) with a stride of 1.

(3) GRU layer: the spatial information captured by the 1D CNN was used as input for the GRU layer to continue the extraction of time-series features from the data. Based on our previous experiences and multiple trials, three GRU layers were used to thoroughly extract features corresponding to the vertical sequences and depth-wise changes of the seismic attributes and well logs. Furthermore, a dropout layer with a dropout parameter of 0.4 was placed after the last GRU layer to prevent overfitting.

(4) Fully connected layer and output layer: a fully connected layer was placed at the end of the network to combine the spatial features extracted by the 1D CNN and sequence features captured by the GRU, thus completing the mapping of spatiotemporal features to porosity logs. The fully connected layer is connected to the output layer, which outputs the predicted porosity values of the network.

3.4 Experimental results and analysis

(1) Reservoir porosity predictions of the 1D CNN–GRU model

The performance of the proposed method was evaluated by performing porosity prediction using the 1D CNN–GRU, 1D CNN, and GRU networks with the nine selected seismic attributes as input. The results are shown in Fig. 8.

Table 4 compares the training and validation errors of the 1D CNN, GRU, and 1D CNN–GRU models in terms

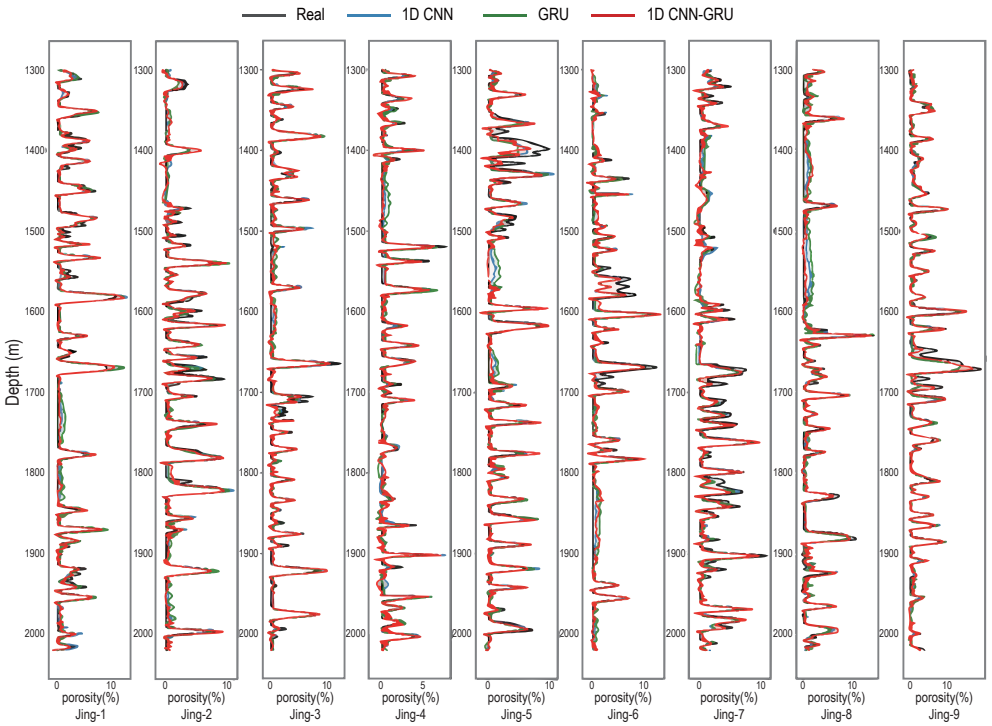

Fig. 8 Comparison of the porosity prediction results.

Table 4 Comparison of the porosity predictions by each model

Network model	Training error		Validating error	
	MAE	RMSE	MAE	RMSE
1D CNN	0.050	0.078	0.052	0.076
GRU	0.038	0.055	0.043	0.053
1D CNN–GRU	0.025	0.042	0.022	0.041

of mean absolute error (MAE) and RMSE to evaluate their predictive performance. The results show that the 1D CNN–GRU model outperforms 1D CNN and GRU in all of these metrics.

Figure 9 shows actual porosity vs. predicted porosity scatter plots for the 1D CNN–GRU, 1D CNN, and GRU models. The 1D CNN–GRU model exhibits considerably better predictive performance than the 1D CNN and GRU models because its predictions have a tighter spread around the diagonal. Furthermore, its accuracy is considerably higher in the high- and low-porosity areas. In summary, the porosity predictions of the 1D CNN–GRU model are considerably closer to the true porosities than those of the 1D CNN and GRU models.

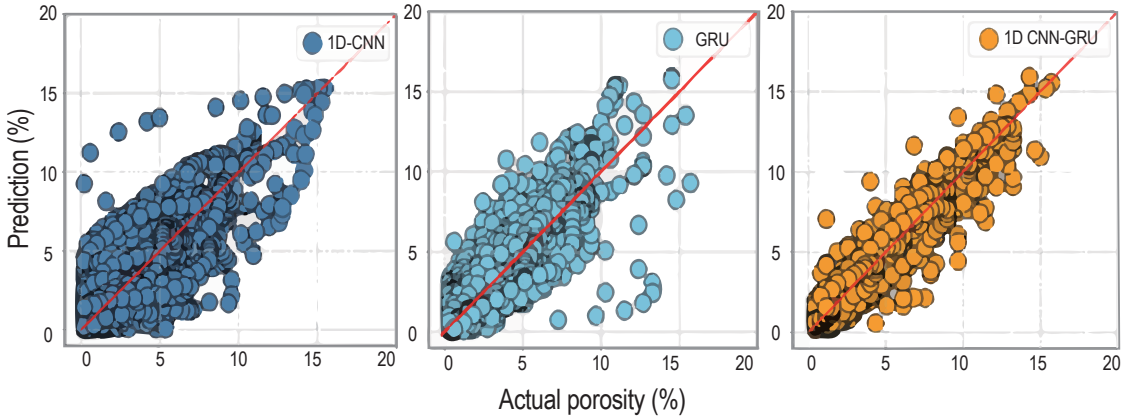

Fig. 9 Comparison of porosity prediction efficacy among the 1D CNN, GRU, and 1D CNN–GRU models.

(2) Prediction of porosity profiles for tight sandstone reservoirs and validation of results

The well log of Jing-12, which was not used for model training or validation, was used as the blind dataset to evaluate the predictive performance and accuracy of the 1D CNN–GRU model. Profile data were extracted along the Xline and Inline directions of Jing-12 and processed (e.g., dimension transformation) to convert the data into suitable inputs for the model. Subsequently, the data were divided into batches to train the network and obtain the porosity profile of Jing-12.

Figures 10 and 11 correspond to the porosity profiles predicted by the 1D CNN–GRU model for Jing-12 in the Inline and Xline directions, respectively. The predicted porosities are a good fit for the porosity log, proving that the predictive performance and accuracy of the 1D

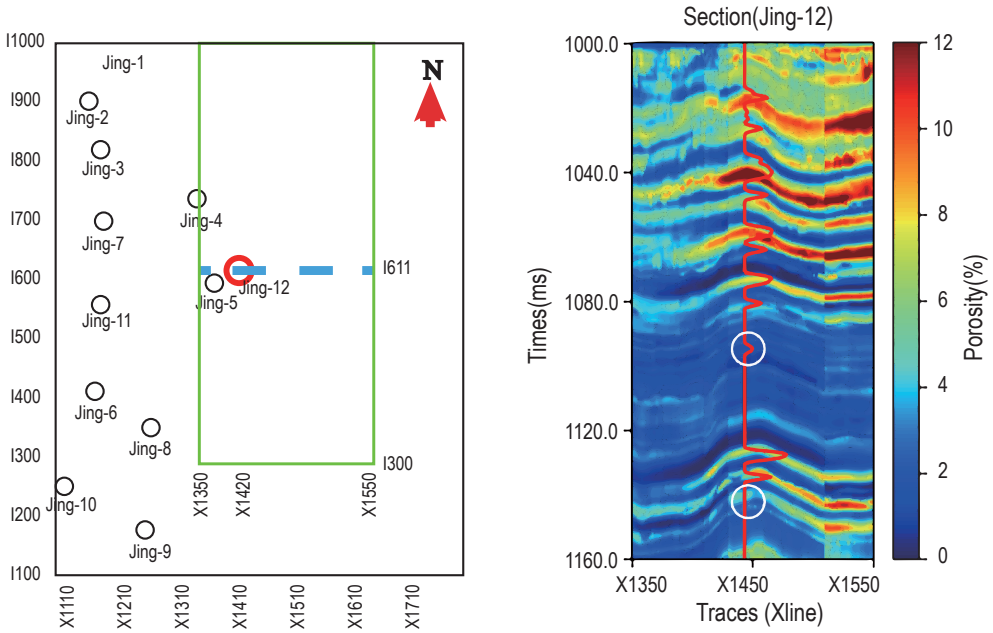

Fig. 10 Porosity profile predicted by the 1D CNN–GRU model for Jing-12 (Xline orientation).

CNN–GRU model are adequate. Furthermore, because the porosity profile predicted by the 1D CNN–GRU shows good continuity in the lateral space, it effectively reveals the shape and extension of the spatial distribution of the tight sandstone reservoir.

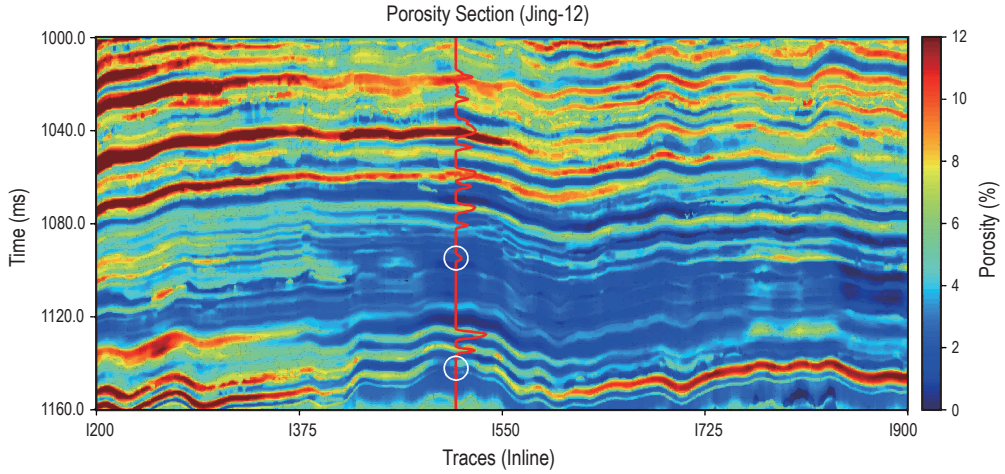

Fig. 11 Porosity profile predicted by the 1D CNN–GRU model for Jing-12 (Inline orientation).

(3) Predicting the 3D porosity volume of the tight sandstone reservoir

Using 3D seismic attribute volumes as input, the 1D CNN–GRU model, which was trained on data from well sites, was extended to nonwell regions. Thus, the 3D porosity volume was predicted for the study area (Fig. 12), revealing the location of the tight sandstone reservoir in the study area and its approximate extension. Therefore, 3D porosity volume predictions by the 1D CNN–GRU model can be used as a reference for studies on tight sandstone reservoirs and their porosities.

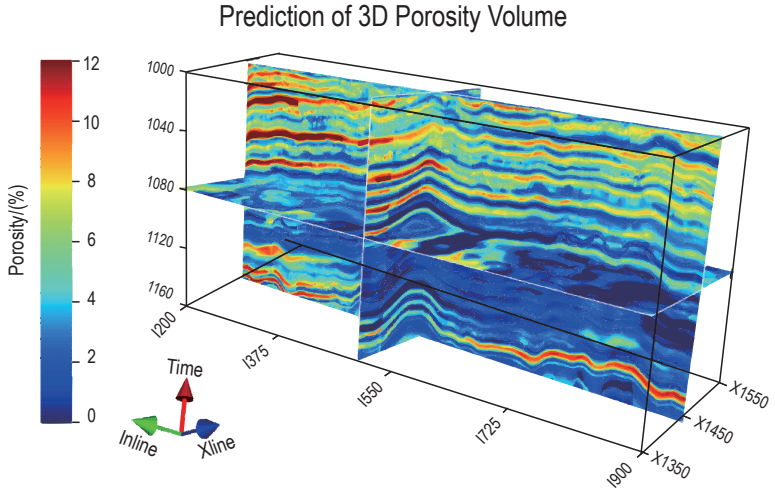

Fig. 12 3D porosity volume predicted by the 1D CNN–GRU model.

Conclusions

a. Because seismic attributes are linked to porosity by complex nonlinear relations that are challenging to identify using conventional means, a Pearson correlation–RF scheme was proposed for selecting the seismic attributes best suited for predicting porosity.

b. Compared to the 1D CNN and GRU models, the proposed 1D CNN–GRU model reduces the predictive error by 50% and 23%, respectively. Therefore, joint model networks hold a considerable advantage over single-model networks in porosity predictions.

c. Combining a 1D CNN network and a GRU network,

we constructed a 1D CNN–GRU model that fuses the vertical and horizontal spatiotemporal features of well log and seismic attribute data. Therefore, the predictions of this model have high resolution in the vertical and horizontal dimensions.

Acknowledgments

We express our heartfelt gratitude to the editors and reviewers for their valuable comments and suggestions.

This research was jointly supported by the Fundamental Research Funds for the Central Universities (No. 2022JCCXMT01) and the Open Fund of State Key Laboratory for Fine Exploration and Intelligent Development of Coal Resources (No. SKLCRSM22DC02).

References

Al-Anazi, A. F. and Gates, I. D., 2012, Support vector regression to predict porosity and permeability: Effect of sample size: Computers & Geosciences, **39** (1), 64–76.

Agbadze, O. K., Qiang, C., and Jiaren, Y., 2022, Acoustic impedance and lithology-based reservoir porosity analysis using predictive machine learning algorithms: Journal of Petroleum Science & Engineering, **208**, 109656.

Al Moqbel, A. and Wang, Y., 2011, Carbonate reservoir characterization with lithofacies clustering and porosity prediction: Journal of Geophysics and Engineering, **8** (4), 592–598.

An, P., Cao, D., Zhao, B., et al., 2019, Reservoir physical parameters prediction based on LSTM recurrent neural network: Progress in Geophysics, **34** (5), 10.

Anh, D. T., Tanim, A. H., Kushwaha, D. P., et al., 2023, Deep learning long short-term memory combined with discrete element method for porosity prediction in gravel-bed rivers: International Journal of Sediment Research, **38** (1), 128–140.

Bakhorji, A., Mustafa, H., Aramco, S., et al., 2012, Rock physics modeling and analysis of elastic signatures for intermediate to low porosity sandstones, 1–5.

Chen, W., Yang, L., Zha, B., et al., 2020, Deep learning reservoir porosity prediction based on multilayer long short-term memory network: Geophysics, **85** (4), WA213–WA225.

Duan, Y., Li, Y., Li, G., et al., 2016, A New Neural Network Model for Rock Porosity Prediction: 2016 International Conference on Identification, Information and Knowledge in the Internet of Things (IIKI), 26–32.

Farquhar, R. A., Somerville, J. M., and Smart, B. G. D., 1994, Porosity as a Geomechanical Indicator: An Application of Core and Log Data and Rock Mechanics: Society of Petroleum Engineers, Richardson, Texas. SPE Paper, 28853, 481–489.

Feng, R., Mejer Hansen, T., Grana, D., et al., 2020, An unsupervised deep-learning method for porosity estimation based on poststack seismic data: Geophysics, **85** (6), M97–M105.

Hampson, D. P., Schuelke, J. S., and Quirein, J. A., 2001, Use of multiattribute transforms to predict log properties from seismic data: Geophysics, **66** (1), 220–236.

Haskett, S. E., Narahara, G. M., and Holditch, S. A., 1988, A Method for Simultaneous Determination of Permeability and Porosity in Low-Permeability Cores: SPE Formation Evaluation, **3** (03), 651–658.

Hamidi, H. and Rafati, R., 2012, Prediction of oil reservoir porosity based on BP-ANN: 2012 International Conference on Innovation Management and Technology Research, 241–246.

Jaf, P., 2015, The Estimation of Porosity and Permeability value for Well TT-4 Through Different Techniques; Well Logging, Well Testing and Core Analysis: Geo Kurdistan II.

Liu, M., Yao, D., Guo, J., et al., 2022, Reservoir Porosity Prediction Model based on Improved Shuffled Frog Leaching Algorithm and BP Neural Network: 2022 7th International Conference on Cloud Computing and Big Data Analytics (ICCCBDA), 62–66.

Na'imi, S. R., Shadizadeh, S. R., Riahi, M. A., et al., 2014, Estimation of Reservoir Porosity and Water Saturation Based on Seismic Attributes Using Support Vector Regression Approach: Journal of Applied Geophysics, **107**, 93–101.

Pramanik, A. G., Singh, V., Vig, R., et al., 2004, Estimation of effective porosity using geostatistics and multiattribute transforms: A case study: Geophysics, **69** (2), 352–372.

Raymer, L. L., Hunt, E. R., Gardner, J. S., 1980, An improved sonic transit time-to-porosity transform: SPWLA Annual Logging Symposium, SPWLA-1980-P.

Saputro, O. D., Maulana, Z. L., and Latief, F. D. E., 2016, Porosity Log Prediction Using Artificial Neural Network: Journal of Physics: Conference Series, **739** (1), 012092.

Shi S., Shi G., Liu Z., et al., 2023, Predicting the water-yield properties of K2 limestones based on multivariate LSTM neural network: A case study of the Poli mining area in Yangquan: Coal Geology & Exploration, **51**(5), 155−163.

Song, J., Ntibahanana, M., Luemba, M., et al., 2023, Ensemble Deep Learning-Based Porosity Inversion From Seismic Attributes: IEEE Access, **11**, 8761−8772.

Srisutthiyakorn, N., 2016, Deep-learning methods for predicting permeability from 2D/3D binary-segmented images: SEG Technical Program Expanded Abstracts 2016, Society of Exploration Geophysicists, 3042–3046.

Wang, J., Cao, J., You, J., et al., 2020, Prediction of reservoir porosity, permeability, and saturation based on a gated recurrent unit neural network: Geophysical Prospecting for Petroleum, **59** (4), 616–627.

Wyllie, M. R. J., Gregory, A. R., Gardner, L. W., 1956, Elastic wave velocities in heterogeneous and porous media: Geophysics, **21** (1), 41–70.

Yang, L., Fomel, S., Wang, S., et al., 2023, Porosity and permeability prediction using a transformer and periodic long short-term network: Geophysics, **88** (1), WA293–WA308.

Zhang, X., Li Q., Li L., et al., 2023, Combination of sonic wave velocity, density and electrical resistivity for joint estimation of gas-hydrate reservoir parameters and their uncertainties: Advances in Geo-Energy Research, **10** (02), 133–140.

Zhang, Z., Zhang, H., Li, J., and Cai, Z., 2021, Permeability and porosity prediction using logging data in a heterogeneous dolomite reservoir: An integrated approach: Journal of Natural Gas Science and Engineering, **86** (1), 103743.

Zhang, Z., Wang, Y., and Wang, P., 2021, On a Deep Learning Method of Estimating Reservoir Porosity: Mathematical Problems in Engineering.

Zou, C., Zhao, L., Xu, M., et al., 2021, Porosity Prediction With Uncertainty Quantification From Multiple Seismic Attributes Using Random Forest: Journal of Geophysical Research: Solid Earth, **126** (7).

Shi Su-zhen, Professor at China University of Mining & Technology-Beijing. Her primary research is seismic interpretation and inversion.

Email: ssz@cumtb.edu.cn